AD-A156 757 FINITE DEFORMATION CRACK-LINE FIELDS IN A THIN ELASTO-PLASTIC SHEET..(U) NORTHWESTERN UNIV EVANSTON IL DEPT OF CIVIL ENGINEERING N NISHIMURA ET AL. FEB 85 NU-SML-TR-85-2 N00014-76-C-0063 F/G 20/11 NL

1/1

UNCLASSIFIED

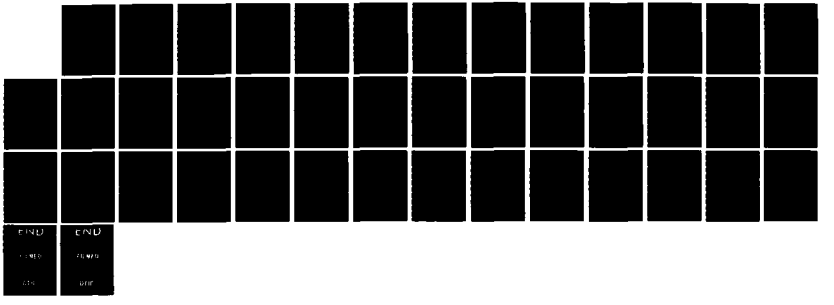

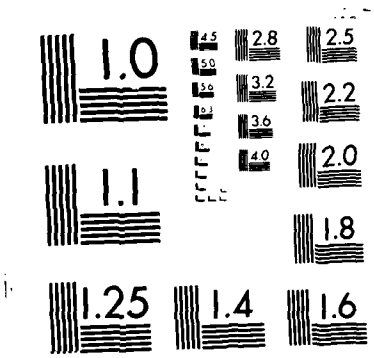

FINITE DEFORMATION CRACK-LINE FIELDS IN A THIN ELASTO-PLASTIC SHEET

N. Nishimura and J. D. Achenbach

Department of Civil Engineering
Northwestern University
Evanston, IL. 60201

Office of Naval Research

NOOO14-76-C-0063

February 1985

NU-SML-TR-No. 85-2

Abstract

Finite deformation in the crack-tip zone of plastic deformation is investigated for Mode-I opening of a crack in a thin sheet of elasto-plastic material. The material obeys the von Mises yield criterion in the true stresses, and the stretching tensor satisfies a flow law of the Prandtl-Reuss type. Incompressibility and a state of generalized plane stress are assumed. It is assumed that linearized elasticity applies outside the zone of plastic deformation. On the crack line between the crack tip and the elastic-plastic boundary, two distinct regions have been recognized: the near tip zone and the intermediate region. In the near tip zone the fields are controlled by the radius of curvature of the blunted crack tip. Here the stress field has been approximated by classical plane stress results. It has been assumed that the crack-line stresses may be taken as uniform in the intermediate region. In each region, deformation variables have been determined by the use of the constitutive relations, and the results have been matched to the corresponding quantities in the neighboring region(s). In this manner expressions have been constructed for the deformation gradients on the crack line, in terms of the distance to the crack tip in the deformed configuration, the yield stress in shear and the stress-intensity factor of linear elastic fracture mechanics.

A-1

Introduction

It is difficult to include the effects of deformation induced geometry changes in an analysis of stresses and deformations near a crack tip. For plane-strain conditions, Rice and Johnson (1970) considered the modification of elasto-plastic crack-tip stress and strain states due to crack blunting. McMeeking (1977) and Rice et al (1979) used finite element methods to include finite deformation in their investigations of crack-tip opening in elastic-plastic materials. Finite deformations near a stationary crack tip in an elastic solid have been investigated by Knowles (1977), Knowles and Sternberg (1980, 1981), and Lo (1977), who used analytical methods.

In this paper we present an approximate analysis of the effect of finite deformation on the crack-line fields for Mode-I opening of a crack in a thin sheet of elasto-plastic material. Away from the crack tips the strains are assumed to be infinitesimal, and the material behaves according to the theory of linear elasticity. The zones of plastic deformation near the crack tips are small as compared to the crack length (small-scale yielding). Finite deformation is, however, taken into account in the near-tip plastic deformation. The constitutive model for the elastic-plastic deformations is a finite deformation version of the elastic perfectly-plastic solid, with the Prandtl-Reuss flow rule and the von Mises yield condition. It is assumed that the material is imcompressible, and that the stress state in the sheet may be approximated by generalized plane stress.

We consider a crack which, in the reference state, is defined by $X_1 < 0$, $X_2 = 0$. The crack faces remain free of surface tractions. In the deformed configuration the stress-equations of equilibrium have the same form as for the corresponding small strain theory. It is assumed that stressing of the sheet gives rise to a blunted crack tip profile of smoothly varying radius of curvature, whose maximum value is reached on the crack line. We focus on

the fields near the crack line, and we consider a near-tip zone and an intermediate region in between the near-tip zone and the elastic-plastic boundary. In the near-tip zone the fields of stress and deformation should be greatly affected by the radius of curvature of the blunted crack tip. In this zone we use a classical stress field that has been applied previously to a sheet containing a circular hole and for a sheet with an edge notch, see Kachanov (1971). This field is axially symmetric. In the intermediate region we assume uniform crack-line stresses. It is to be expected that the actual stresses near the crack line will develop a dependence on the polar angle in the transition from the essentially axisymmetric field very close to the blunted tip to the uniform field in the intermediate region. For simplicity we have,however, assumed that the axisymmetric field remains applicable until it can be matched to the uniform stresses in the intermediate region. The choice of the stress-field in the intermediate region is shown to be consistent with a slip-line field proposed by Thomason (1979).

When the stress fields have been chosen, the crack line deformation can be analyzed by the use of the constitutive relations. The deformation gradients can be solved rigorously in the near-tip zone in terms of a single function of the crack-tip radius, whose form is subsequently determined by matching deformation variables to corresponding ones in the intermediate region. In the latter region the crack-line deformation is analyzed by following the method discussed by Achenbach and Dunayevsky (1984) and Achenbach and Li (1984). The solution is completed by matching the intermediate-region results to the deformation gradients at the elastic-plastic boundary.

The principal results of the paper are expressions for the deformation gradients in terms of the distance to the crack tip in the deformed configuration, the yield stress in shear and the stress intensity factor of linear elastic fracture mechanics. It is shown that $\partial x_2/\partial X_2$ is singular at the crack tip, while $\partial x_1/\partial X_1$ vanishes at that point.

1. Governing Equations

The reference and current positions are defined by postion vectors $\underset{\sim}{X}$ and $\underset{\sim}{x}$, respectively. In the current configuration the equilibrium equation is

$$\text{div}\underset{\sim}{T} = \underset{\sim}{0} \ , \tag{1.1}$$

where $\underset{\sim}{T}$ is the Cauchy stress. In this paper, the spatial derivatives are with respect to $\underset{\sim}{x}$ unless stated otherwise. The constitutive model that is being considered is a large deformation version of the elastic perfectly-plastic solid, with the Prandtl-Reuss flow rule and the von Mises yield criterion. In addition it is assumed that the material is incompressible.

The yield condition is represented by

$$\underset{\sim}{T}' \cdot \underset{\sim}{T}' = 2k^2 \ , \tag{1.2}$$

where k is the yield stress in pure shear and $\underset{\sim}{T}'$ is the stress deviator defined by

$$\underset{\sim}{T}' = \underset{\sim}{T} - \frac{1}{3} \underset{\sim}{I} \ \text{tr}\underset{\sim}{T} \ , \tag{1.3}$$

Here $\underset{\sim}{I}$ and tr stand for the unit tensor and the trace, respectively. When (1.2) is satisfied, we use an incremental constitutive equation of the type

$$\underset{\sim}{D} = \frac{1}{2\mu} \left(\overset{\circ}{\underset{\sim}{T}} + \dot{p}\underset{\sim}{I} \right) + \dot{\Lambda}\underset{\sim}{T}' \ . \tag{1.4}$$

The elastic part of $\underset{\sim}{D}$ is represented by

$$\underset{\sim}{D}^{el} = \frac{1}{2\mu} \left(\overset{\circ}{T} + \dot{p}\underset{\sim}{I} \right) \ . \tag{1.5}$$

Here $\underset{\sim}{D}$ represents the stretching tensor, which is defined by

$$\underset{\sim}{D} = \frac{1}{2} [\underset{\sim}{\nabla v} + (\underset{\sim}{\nabla v})^T] , \tag{1.6}$$

where $\underset{\sim}{v}$ is the particle velocity:

$$\underset{\sim}{v} = \dot{\underset{\sim}{x}} = \frac{\partial \underset{\sim}{x}}{\partial t} (\underset{\sim}{X}(\underset{\sim}{x},t),t) . \tag{1.7}$$

The dot symbol denotes the material time derivative. In (1.4) and (1.5) p defines the indeterminate pressure, $\dot{\Lambda}$ a positive multiplier, and the $^\circ$ symbol defines the Jaumann rate:

$$\overset{\circ}{\underset{\sim}{T}} = \dot{\underset{\sim}{T}} - \underset{\sim}{WT} + \underset{\sim}{TW} , \tag{1.8}$$

where

$$\underset{\sim}{W} = \frac{1}{2} [\underset{\sim}{\nabla v} - (\underset{\sim}{\nabla v})^T] . \tag{1.9}$$

It should be noted that there is some controversy over the choice of stress rate in rate-type constitutive equations, see e.g. Lee et al (1983) and Dienes (1979). If one wishes to rewrite a small deformation constitutive equation of rate type into its large deformation counterpart just by replacing the small deformation stress rate by an objective stress rate, it is, to the present authors' opinion, generally inadvisable to use the Jaumann rate. This is because $\underset{\sim}{W}$ is not a measure of the rate of rotation of a material point. Indeed, it is not difficult to find a deformation gradient $\underset{\sim}{F}$ which is symmetric positive definite (rotation - free with regard to polar decomposition), but with non-zero $\underset{\sim}{W}$. Actually

$$\underset{\sim}{F} = \underset{\sim}{Q}(t)\underset{\sim}{\Gamma}\underset{\sim}{Q}^T(t) \tag{1.10}$$

provides such an example, where $\underset{\sim}{Q}(t)$ is a time dependent orthogonal tensor, and $\underset{\sim}{\Gamma}(\neq \gamma \underset{\sim}{I}, \gamma = \text{const.})$ is a symmetric positive definite constant tensor. From the physical point of view, it seems that in the constitutive equations (1.4) and (1.5) , Dienes' rate, Dienes (1979), is a more reasonable choice than Jaumann's rate. In the present analysis, however, the use of Jaumann's rate is acceptable because the principal axes of stress do not rotate significantly. In addition, Jaumann's rate is much easier to handle than other rates. These are the reasons for using (1.4) and (1.5) here.

The pressure p can be eliminated from (1.4) and (1.5) by using the condition of incompressibility

$$\text{div } \underset{\sim}{v} = 0 \ . \tag{1.11}$$

By taking the trace of (1.4) or (1.5) we obtain

$$\dot{p} = -\frac{1}{3} \text{ tr } \overset{\circ}{\underset{\sim}{T}} \quad , \tag{1.12}$$

which in turn reduces (1.4) to

$$\underset{\sim}{D} = \frac{1}{2\mu} \left(\overset{\circ}{\underset{\sim}{T}} - \frac{1}{3} \underset{\sim}{I} \text{ tr } \overset{\circ}{\underset{\sim}{T}} \right) + \dot{\Lambda} \underset{\sim}{T}' \quad , \tag{1.13}$$

In the present paper we will discuss the deformations of a thin cracked sheet of uniform initial thickness h. As in the corresponding small deformation theory, one can facilitate the analysis by using the generalized plane-stress assumption. To see the implication of this assumption we introduce a Cartesian coordinate system with its $x_3 = 0$ plane coinciding with the mid-plane of the undeformed sheet. Under the assumptions that the

deformation is symmetric with respect to the mid-plane, that the 1st Piola Kirchhoff stress does not vary significantly throughout the thickness, and that the planer faces are free of loads, Knowles and Sternberg (1983) showed that

$$T_{\alpha 3} = T_{3\alpha} = 0 \ , \quad F_{3\alpha} = F_{\alpha 3} = 0 \ , \quad T_{33} = 0 \tag{1.14a,b,c}$$

hold on $x_3 = 0$, where Greek indices stand for either 1 or 2. If (1.14a) holds not just on $x_3 = 0$ but in its vicinity, we may reduce (1.1) to its 2D version, i.e.,

$$T_{\alpha\beta,\beta} = 0 \ . \tag{1.15}$$

This equation and (1.2) constitute the governing equations for the stress components. It is noted that the same equations govern the stress distributions in the theory of small-strain plane-stress plasticity. Therefore, we may utilize some known results from that theory. Another implication of the plane stress assumption is that

$$v_{3,\alpha} = v_{\alpha,3} = 0, \quad (x_3 = 0). \tag{1.16}$$

With this result and the constitutive equations (1.13), we can determine the velocity field in the mid-plane.

2. Crack-Line Stresses

We start with the observation that the equilibrium equation (1.15) and the yield condition (1.2) have the same form as for small deformation theory, except that in the present context the stress is referred to the $\underset{\sim}{x}$ position (after deformation). Therefore the classical plane stress analysis for stresses applies to the present problem, but with the boundary conditions imposed on deformed boundaries.

It is assumed that the crack tip will blunt into a curve S which has a root radius whose magnitude attains its maximum value a on the crack line. For small polar angles, we may then approximate S by a segment of a circle C of radius a.

At this point, we recall some formulas from the classical theory of plane stress plasticity, see e.g. Kachanov (1971), pp. 262-272. A set of principal stresses

$$T_1 = 2k\cos(\omega - \tfrac{1}{6}\pi), \quad T_2 = 2k\cos(\omega + \tfrac{1}{6}\pi), \quad (0 \leq \omega \leq \pi), \tag{2.1a,b}$$

satisfies the yield condition (1.2), where ω is a parameter. When $\pi/6 < \omega < 5\pi/6$, the equilibrium equation becomes hyperbolic. The equations for the characteristics and the corresponding integrals are:

α - characteristics

$$\frac{dx_2}{dx_1} = \tan(\phi-\psi), \quad \Omega - \phi = \text{const}, \tag{2.2a,b}$$

β - characteristics

$$\frac{dx_2}{dx_1} = \tan(\phi+\psi), \quad \Omega + \phi = \text{const}, \tag{2.3a,b}$$

where ϕ is the angle between the T_1 and x_1 directions,

$$\psi(\omega) = \frac{1}{2}\pi - \frac{1}{2}\arccos\left(\frac{\cot\omega}{\sqrt{3}}\right) , \tag{2.4}$$

and

$$\Omega(\omega) = -\frac{1}{2}\int_{\pi/6}^{\omega} \frac{(3-4\cos^2\xi)^{\frac{1}{2}}}{\sin\xi}\, d\xi . \tag{2.5}$$

With regard to the crack-line stresses, one would expect that the stress right near the tip is affected by the traction free boundary S, while the stress away from the tip (but still within the plastic zone) will not be all that different in form from those for the corresponding small-strain crack problems. This would suggest that we should approximate the crack-line stresses by using two fields: one for the immediate vicinity of the crack tip, and another for the intermediate region between the near-tip zone and the elastic-plastic boundary.

2.1 Stresses in the near-tip zone

Let A and B be points on S between which C and S do not differ significantly, see Fig. 1. Also, let $\mathcal{D}$ be a domain surrounded by the arc AB, and two characteristics defined by (2.3) and (2.2), emanating from A and B. It is reasonable to approximate S between A and B by C . Then the stresses in $\mathcal{D}$ are found as solutions of the equilibrium equation (1.15) and the yield condition (1.2) subject to

$$T_r = 0 , \quad T_{r\theta} = 0 \quad \text{on } r = a , \tag{2.6}$$

where T_r, T_θ, and $T_{r\theta}$ stand for the components of $\underset{\sim}{T}$ referred to the polar

coordinate system (r,θ) which has its origin at the center of C. Due to the hyperbolicity of the governing equation, $T_{r\theta}$ vanishes identically within $\mathcal{D}$, and T_r and T_θ show axisymmetry. The solution to this problem appears in standard textbooks of plasticity in connection with the extension of a sheet with a circular hole. We record the following results from Kachanov (1971):

$$\left(\frac{r}{a}\right)^2 = \frac{\sqrt{3}}{2\sin\omega}\, e^{\sqrt{3}(\pi/3-\omega)} \quad , \tag{2.7a}$$

$$T_r = 2k\cos\left(\omega + \frac{\pi}{6}\right) \quad , \quad T_\theta = 2k\cos\left(\omega - \frac{\pi}{6}\right) \qquad (0 < \omega < \pi/3) \quad . \tag{2.7b,c}$$

2.2 Crack-line stresses in the intermediate region

Two Mode-I near-tip stress distributions have been proposed for the small-deformation plane-stress case in an elastic perfectly-plastic material. Hutchinson (1968) proposed a stress field which corresponds to the system of characteristic curves shown in Fig. 2. He also showed that this distribution can be obtained as the limit for a certain non-linear elastic material as the stress-strain curve becomes flat. In the loading zone ahead of the crack tip the stresses are

$$T_{11} = k\cos^3\theta, \quad T_{22} = k(2\cos^3\theta + 3\sin^2\theta\cos\theta), \quad T_{12} = -k\sin^3\theta. \tag{2.8a,b,c}$$

The crack line stresses are $T_{11} = k$, $T_{22} = 2k$ and $T_{12} = 0$. The latter results also follow from (2.1), since it can be deduced from (2.2)-(2.4) and Fig. 2 that the crack line is a characteristic curve with $\omega = \pi/6$.

Thomason (1979) proposed a class of stress fields which include the Hutchinson field as a special case. The system of characteristic curves is

$$F(a) = \frac{\eta}{F_1}\, a \ . \tag{5.11}$$

Substitution of (5.11) into (3.28) - (3.30) completes the desired relations on the crack line in the near-tip zone, $a < x_1 < \kappa a$. In the intermediate region, $\kappa a < x_1 < x_p$, we find from (5.11), (5.7) and (3.28)

$$X_1 = \frac{1}{F_1}\,(x_1 - \sqrt{3}a/\kappa) \ . \tag{5.12}$$

By using (4.13), (5.2), (5.1) and the previously computed result for C(t), the expression for $v^*_{2,2}$ becomes

$$v^*_{2,2} = \frac{\sqrt{3}\dot{a}}{\kappa^3 a^2}\,\frac{1+\delta}{1-\delta}\left(\frac{\sqrt{3}}{\kappa}\,a + x_o\right) - \frac{2\sqrt{3}\dot{a}}{\kappa^2 a}\,\frac{\delta}{1-\delta} \ . \tag{5.13}$$

For $\kappa a < x_1 < x_p$, (4.14) then takes the form

$$\frac{\partial x_2}{\partial X_2} = F(x_o)[a/G^*(x_o)]^p\, e^{-qx_o[1/a-1/G^*(x_o)]} \ , \tag{5.14}$$

where

$$p = \frac{3(1+\delta) - 2\sqrt{3}\kappa^2\delta}{\kappa^4(1-\delta)} \ , \tag{5.15}$$

$$q = \frac{\sqrt{3}(1+\delta)}{\kappa^3\,(1-\delta)} \ , \tag{5.16}$$

and

$$G^*(x_o) = \int_o^{G(x_o)} \dot{a}\,dt \ . \tag{5.17}$$

The function $G^*(x_o)$ may be selected in a convenient manner since $G(x_o)$ is arbitrary, see also the footnote under Eq.(4.12).

$$X_1 = F(x_o/\eta) \ . \tag{5.7}$$

Differentiation of this expression gives

$$x_2 = 0 \ , \quad \kappa a < x_1 < x_p : \quad \frac{\partial x_1}{\partial X_1} = \frac{\eta}{F'(x_o/\eta)} \ , \tag{5.8}$$

where $x_1 = x_p$ defines the elastic-plastic boundary.

At the elastic plastic boundary the deformation gradients are F_1 and F_2, i.e.,

$$\left(\frac{\partial x_1}{\partial X_1} \ , \ \frac{\partial x_2}{\partial X_2}\right) = (F_1, F_2) \ . \tag{5.9}$$

It can be shown that both $\partial x_1/\partial X_1$ and $\partial x_2/\partial X_2$ are continuous across $x_1 = x_p$. The uniformity of T_{11} and T_{22} in the intermediate zone also implies that F_1 and F_2 depend on k and the elastic constants only, i.e. F_1 and F_2 are independent of a. Equations (5.8) and (5.9) then give the relation

$$\text{at } x_1 = x_p : \quad F'\left(\frac{x_1 - \sqrt{3}a/\kappa}{\eta}\right) = \frac{\eta}{F_1} \ , \tag{5.10}$$

where (5.4) has also been used. The argument of $F'(\cdot)$ depends on a, but the right-hand side of the equation is independent of a. It then follows that $F(\cdot)$ is either linear in its argument, or the argument is constant. The latter case would be $x_p - \sqrt{3}a/\kappa = \text{constant}$. Since the plastic zone should vanish as $a \to 0$, the constant must be zero, implying $x_p < a$, which is unacceptable. Hence (5.10) can only give a linear relation for $F(\cdot)$. The integration constant has been set equal to zero, because $x_p \to 0$ as $a \to 0$. If we would take a as the argument we can write

5. Matching of Solutions

It may be assumed that the particle velocities as well as their derivatives with respect to x_2 are continuous at $x_1 = \kappa a$ on the crack line. It then follows from (3.18a) and (4.3b) that for $\kappa a < x_1 < x_p$, $x_2 = 0$

$$v_1 = \frac{\sqrt{3}}{\kappa} \dot{a} \ . \tag{5.1}$$

Equations (4.4b) and (3.18c) yield

$$v_{1,22} = - \frac{\sqrt{3}}{\kappa^3} \frac{\dot{a}}{a^2} \ . \tag{5.2}$$

The function C(t) follows by matching (4.6) to (3.18b). Equation (4.6) may then be written as

$$v_{2,2} = \frac{\sqrt{3}\dot{a}}{\kappa^3 a^2} \frac{1+\delta}{1-\delta} x_1 - \frac{2\sqrt{3}\ \dot{a}}{\kappa^2 a} \frac{\delta}{1-\delta} \ . \tag{5.3}$$

With (5.1) and the assumption that $a = 0$ at $t = 0$, we may rewrite (4.9) as

$$x_o = x_1 - \frac{\sqrt{3}}{\kappa} a \ , \tag{5.4}$$

and hence (4.8) becomes

$$X_1 = X_o \ (x_1 - \sqrt{3}a/\kappa) \ . \tag{5.5}$$

Continuity of X_1 at $x_1 = \kappa a$ then yields the identity

$$F(a) = X_o(\eta a) \ , \quad \eta = \kappa - \sqrt{3}/\kappa \ , \tag{5.6a,b}$$

where (3.28) and (5.5) have been used. Equations (5.6a) and (5.5) now imply

Here F and G are arbitrary functions,† and $v^*_{2,2}(s,x_o)$ follows from (4.6) and (4.9) as

$$v^*_{2,2}(s,x_o) = -\frac{1+\delta}{1-\delta} v_{1,22}(s) \left(\int_o^s v_1(t)dt + x_o \right) + C(s) . \tag{4.13}$$

From (4.11) we conclude that on the crack line

$$\frac{\partial x_2}{\partial X_2} = F(x_o)\, e^{h(t,x_o)} . \tag{4.14}$$

In the next section the functions $v_1(t)$, $v_{1,22}(t)$, $x_o(x_1,t)$, $C(t)$, $F(x_o)$, $X_o(x_o)$ and $G(x_o)$ will be determined by the use of appropriate matching conditions.

† One of these functions is actually redundant, but the form (4.11) is convenient for later use.

or

$$v_{2,2} = - \frac{1+\delta}{1-\delta} v_{1,22}(t)x_1 + C(t) , \tag{4.6}$$

where δ is defined by (3.11), and $C(t)$ is an arbitrary function.

With these results, one can relate $\underset{\sim}{X}$ to $\underset{\sim}{x}$. Indeed, since $\dot{\underset{\sim}{X}} \equiv \underset{\sim}{0}$, we have

$$\frac{\partial X_1}{\partial t} + v_1 \frac{\partial X_1}{\partial x_1} = 0 , \tag{4.7}$$

where we have used that $v_2 \equiv 0$ on the crack line. Equation (4.7) yields

$$X_1 = X_o(x_o) , \tag{4.8}$$

where X_o is an arbitrary function and x_o is defined by

$$x_o = x_1 - \int_o^t v_1(s)ds. \tag{4.9}$$

To determine an expression for $\partial x_2/\partial X_2$ on the crack line, we use $(\partial/\partial x_2)(\dot{X}_2) = 0$, to obtain

$$\frac{\partial}{\partial t}\left(\frac{\partial X_2}{\partial x_2}\right) + v_1 \frac{\partial}{\partial x_1}\left(\frac{\partial X_2}{\partial x_2}\right) = - v_{2,2} \frac{\partial X_2}{\partial x_2} , \tag{4.10}$$

where we have used that $v_2 \equiv 0$ and $X_2 \equiv 0$ on the crack line. The solution to (4.10) is

$$\frac{\partial X_2}{\partial x_2} = \frac{1}{F(x_o)} e^{-h(t,x_o)} , \tag{4.11}$$

where

$$h(t,x_o) = \int_{G(x_o)}^t v^*_{2,2}(s,x_o)ds. \tag{4.12}$$

4. Crack-Line Deformation in the Zone of Uniform Stress

Next we investigate the crack-line displacement gradients away from the tip, in the region where the stresses are defined by (2.10), i.e., $T_{11} = k$ and $T_{22} = 2k$. We essentially follow the procedure proposed by Achenbach and Li (1984).

Substitution of (2.10) into (1.8) and (1.3) gives near the crack-line:

$$\overset{\circ}{\underset{\sim}{T}} = \frac{1}{2}\,(v_{1,2} - v_{2,1}) \begin{pmatrix} 0 & -k & 0 \\ -k & 0 & 0 \\ 0 & 0 & 0 \end{pmatrix} , \tag{4.1a}$$

$$\underset{\sim}{T}' = \begin{pmatrix} 0 & 0 & 0 \\ 0 & k & 0 \\ 0 & 0 & -k \end{pmatrix} . \tag{4.1b}$$

Equation (1.13) then yields

$$\underset{\sim}{D} = \frac{1}{4\mu}\,(v_{1,2}-v_{2,1}) \begin{pmatrix} 0 & -k & 0 \\ -k & 0 & 0 \\ 0 & 0 & 0 \end{pmatrix} + \dot{\Lambda} \begin{pmatrix} 0 & 0 & 0 \\ 0 & k & 0 \\ 0 & 0 & -k \end{pmatrix} . \tag{4.2}$$

Since $D_{11} \equiv 0$, we have on the crack line

$$v_{1,1} = 0 , \quad \text{or} \quad v_1 = v_1(t) . \tag{4.3a,b}$$

Equation (4.3a) also holds near the crack line, and hence we may write for $x_2 = 0$, $-\infty < a < x_1$

$$v_{1,221} = 0 , \quad \text{or} \quad v_{1,22} = v_{1,22}(t) . \tag{4.4a,b}$$

In the same manner $(\partial/\partial x_2)D_{12}$ yields for $x_2 = 0$, $-\infty < a < x_1$:

$$(1+\delta)\, v_{1,22} = -\,(1-\delta)\, v_{2,21} , \tag{4.5}$$

Equation (3.25) implies

$$R = F(ae^{-g(\rho)}) \ , \tag{3.27}$$

where the functional form $F(\cdot)$ will be determined in the sequel. Since the displacement is radial it follows from (3.27) that

$$X_\alpha = \frac{x_\alpha}{r} F(ae^{-g(\rho)}) \ , \tag{3.28}$$

where $g(\rho)$ is defined by (3.26). Differentiation of (3.28) yields

$$\frac{\partial X_\alpha}{\partial x_\beta} = \frac{1}{r}\left(\delta_{\alpha\beta} - \frac{x_\alpha x_\beta}{r^2}\right) F(ae^{-g(\rho)}) + \frac{x_\alpha x_\beta}{r^2} F'(ae^{-g(\rho)}) \frac{e^{-g(\rho)}}{\rho - f(\rho)} \ . \tag{3.29}$$

On the crack line at $r = \kappa a$ we have

$$\frac{\partial x_1}{\partial X_1} = \frac{\kappa - f(\kappa)}{F'(a)} \ , \quad \frac{\partial x_2}{\partial X_2} = \frac{\kappa a}{F(a)} \ , \quad \frac{\partial x_1}{\partial X_2} = \frac{\partial x_2}{\partial X_1} \equiv 0. \tag{3.30a,b,c}$$

Equation (3.13) or (3.15), together with (2.7a) and (3.4a),determine the velocity field near the tip.

We next determine the relation between $\underset{\sim}{x}$ and $\underset{\sim}{X}$. To this end, we note that

$$\dot{R} = \frac{\partial R}{\partial t} + v_\alpha \frac{\partial R}{\partial x_\alpha} = 0 \tag{3.19}$$

holds, where

$$R = (X_\alpha X_\alpha)^{\frac{1}{2}}. \tag{3.20}$$

Equation (3.19) implies that R = const on

$$\frac{dx_\alpha}{dt} = v_\alpha \ , \tag{3.21}$$

or

$$\frac{dr}{da} = f(\rho) \ , \tag{3.22}$$

where we have used (3.4a,b) and changed the independent variable from t to a. It is more convenient to use $\rho = r/a$ instead of a in (3.22). Noting the relation

$$\frac{da}{d\rho} = \frac{1}{\rho}\frac{dr}{d\rho} - \frac{r}{\rho^2} \ , \tag{3.23}$$

we transform (3.22) into

$$\frac{dr}{d\rho} = -\frac{f(\rho)\ r}{\rho[\rho - f(\rho)]} \ , \tag{3.24}$$

which integrates to

$$r/r_o(R) = \rho\ e^{\,g(\rho)} \ , \tag{3.25}$$

where $r_o(R)$ is an arbitrary function of R, and

$$g(\rho) = \int_\rho^\infty \frac{d\zeta}{\zeta - f(\zeta)} \ . \tag{3.26}$$

where (3.4a) has been used. The exact solution to (3.10) and (3.12) can easily be written out:

$$f(\omega) = \frac{e^{-\pi/2\sqrt{3}}}{(2/\sqrt{3})^{\frac{1}{2}}} \frac{e^{\omega\sqrt{3}/2}}{(\sin\omega)^{\frac{1}{2}}} \left[\frac{1-\sin(\omega-\pi/3)}{\cos(\omega-\pi/3)}\right]^{\delta} \left\{1 - \delta e^{\pi/\sqrt{3}} I_1(\omega)\right\} , \tag{3.13}$$

where

$$I_1(\omega) = \int_{\omega}^{\pi/3} \frac{e^{-\xi\sqrt{3}} d\xi}{\cos^{1-\delta}(\xi-\pi/3)[1-\sin(\xi-\pi/3)]^{\delta}} . \tag{3.14}$$

When δ is small, which is usually the case, this solution reduces to

$$f(\omega) = \frac{e^{-\pi/2\sqrt{3}}}{(2/\sqrt{3})^{\frac{1}{2}}} \frac{e^{\omega\sqrt{3}/2}}{(\sin\omega)^{\frac{1}{2}}} . \tag{3.15}$$

This expression satisfies (3.12). At the boundary of the near-tip zone, i.e. for $\omega = \pi/6$ and $r = \kappa a$ we find

$$f(\omega = \pi/6) \equiv f(\rho = \kappa) = \sqrt{3}/\kappa , \tag{3.16}$$

where κ is defined by (2.9).

Equation (3.15) together with (2.7a) and (3.4a) determines the velocity field in the near-tip zone. For future reference we list the following results, which follow from (3.4a,b) :

$$v_{2,2} = \frac{\dot{a}}{a} \frac{f(\rho)}{\rho} , \quad v_{1,22} = \frac{\dot{a}}{a^2} \frac{f'(\rho)\rho - f(\rho)}{\rho^2} . \tag{3.17a,b}$$

Using the result (3.16) we find at $r = \kappa a$:

$$v_1 = \frac{\sqrt{3}\dot{a}}{\kappa} , \quad v_{2,2} = \frac{\sqrt{3}\dot{a}}{\kappa^2 a} , \quad v_{1,22} = -\frac{\sqrt{3}\dot{a}}{\kappa^3 a^2} . \tag{3.18a,b,c}$$

Since $\underset{\sim}{W}$ vanishes identically, we have

$$\overset{\circ}{\underset{\sim}{T}} = \dot{\underset{\sim}{T}} = \dot{a}\,\frac{\partial}{\partial a}\,\underset{\sim}{T} + v_\alpha\,\frac{\partial}{\partial X_\alpha}\,\underset{\sim}{T} \quad . \tag{3.5}$$

By the use of (3.5), (3.4 c-f) and (1.13) we obtain equations for $\partial v_r/\partial r$ and v_r/r. Subsequent use of (3.4) reduces these equations to

$$f'(\rho) = \frac{1}{6\mu}\,[f(\rho)-\rho](2T_r' - T_\theta') + \lambda\left(\frac{2}{3}\,T_r - \frac{1}{3}\,T_\theta\right) \quad , \tag{3.6}$$

$$\frac{f(\rho)}{\rho} = \frac{1}{6\mu}\,[f(\rho)-\rho](-T_r' + 2T_\theta') + \lambda\left(\frac{2}{3}\,T_\theta - \frac{1}{3}\,T_r\right) \quad . \tag{3.7}$$

In (3.6) - (3.7), a prime denotes a derivative with respect to ρ. Elimination of λ from (3.6) and (3.7) yields after some additional manipulation

$$f'(\rho) - \frac{2T_r-T_\theta}{2T_\theta-T_r}\,\frac{f(\rho)}{\rho} + \frac{1}{2\mu}\,\frac{T_\theta'T_r-T_r'T_\theta}{2T_\theta-T_r}\,[f(\rho)-\rho] = 0. \tag{3.8}$$

According to (2.7a), ρ and ω are related by

$$\rho(\omega) = \frac{e^{\pi/2\sqrt{3}}}{(2/\sqrt{3})^{\frac{1}{2}}}\;\frac{e^{-\omega\sqrt{3}/2}}{(\sin\omega)^{\frac{1}{2}}} \quad . \tag{3.9}$$

Elimination of ρ from (3.8) by the use of (3.9) then yields

$$\frac{df}{d\omega} + \left[\frac{\cos(\omega+\pi/3)}{\sin\omega} + \frac{\delta}{\cos(\omega-\pi/3)}\right] f = \frac{\delta\rho(\omega)}{\cos(\omega-\pi/3)} \quad , \tag{3.10}$$

where

$$\delta = k/2\mu \quad . \tag{3.11}$$

The boundary condition (3.3) on r = a reduces to

$$f(\pi/3) = 1 \quad , \tag{3.12}$$

3. Crack-Line Deformation in the Near-Tip Zone

In this Section the displacement gradients are determined on the crack line in the near-tip zone defined by $a < x_1 < \kappa a$. First we analyze the velocity vector $\underset{\sim}{v}$ by integrating (1.13) with an appropriate condition at $r = a$. Since we have assumed that near the crack line the deformed crack-tip boundary may be approximated by a circular segment of radius a, we have

$$x_\alpha x_\alpha = a^2. \tag{3.1}$$

The components of the particle velocity then satisfy

$$v_\alpha x_\alpha = a\dot{a} \ , \quad \text{on } |\underset{\sim}{x}| = a \ , \tag{3.2}$$

but are arbitrary otherwise. To simplify the analysis we assume that $\underset{\sim}{v}$ is radial, i.e.,

$$v_\alpha = \frac{\dot{a}}{a} x_\alpha \qquad \text{on } |\underset{\sim}{x}| = a \ . \tag{3.3}$$

Then, the velocity field inside the material also becomes radial due to the hyperbolicity of the governing operation. This justifies the introduction of the following forms:

$$v_r = \dot{a}\, f(\rho) \ , \quad v_\theta = 0 \ , \tag{3.4a,b}$$

$$T_r = T_r(\rho) \ , \quad T_\theta = T_\theta(\rho) \ , \quad T_{r\theta} = 0 \ , \tag{3.4c,d,e}$$

$$\dot{\Lambda} = \frac{\dot{a}}{a}\ \lambda(\rho) \ , \tag{3.4f}$$

where $\rho = r/a$, $r = \sqrt{(x_\alpha x_\alpha)}$, and $f(\rho)$ and $\lambda(\rho)$ are functions of ρ, and $T_r(\rho)$ and $T_\theta(\rho)$ are the stress components computed from (2.7b,c).

reason we have selected the Thomason field for the intermediate region. As discussed earlier, however, the apex angle α of uniform field has to be small. It can be shown that the point A', where the solution (2.7) is connected to a uniform field, has an x_1 coordinate smaller than κa. Since the system of Fig. 4 reduces to that of Fig. 5 in the limit of $\alpha \to 0$ we may assume that the x_1 coordinate of A' can be approximated as κa for small α. Accordingly, one may say that the stress near the crack line beyond A' is uniform and approximately equal to

$$T_{11} = k \quad T_{22} = 2k \quad \text{for } x_1 > \kappa a, \ |x_2| \sim \text{small}. \tag{2.10}$$

In summary, we will use (2.7) for $a < x_1 < \kappa a$, and (2.10) for $\kappa a < x_1 < x_p$, where x_p is the x_1 coordinate of the elastic-plastic boundary on the crack line.

analytical methods. Consistent with the approximate nature of the present analysis, we will use the simple 'extension' stated above.

To discuss the matching of the stress fields more closely, we examine in a qualitative manner how the characteristics of the fields away from the tip can be combined with those of the near-tip region. Figures 4 and 5 show such combined systems of characteristics for the Hutchinson and Thomason fields, respectively. To the left of the characteristics merging at points A and A' the stress field given by (2.7) is assumed to develop, while we assume Hutchinson's and Thomason's field to the right in Figs. 4 and 5, respectively. In Fig. 4 the crack line is characteristic to the right of point A. Hence the upper and lower characteristics merge at A without slope discontinuity, thus forming a cusp at point A (which, it may be noted, has an x_1 coordinate of κa). From this observation, we may infer (and can prove) that the stress at point A has essentially the same mathematical structure as the Hutchinson field (Fig. 2) has at its origin (the crack tip). This consideration and the analysis by Achenbach and Li (1984) then suggest that the system of characteristic lines shown in Fig. 4 lead to an anomalous deformation having a singularity at A. The details will not be given here, but they can be shown by using the same method as reported in the sequel. Since a deformation singularity at A would be unacceptable we are left with the system of Fig. 5. Due to the presence of the uniform field to the left of the point A' the two characteristics merging at A' will not form a cusp, and, hence, will not cause an unacceptable singularity there. For that

shown in Fig. 3. The essential difference with Fig. 2 is in the presence of a uniform field in a wedge-like region occupying $0 < \theta < \alpha$. Away from this wedge-like region the two fields are essentially the same. Indeed, the field of Fig. 3 reduces to that of Hutchinson as α tends to zero. For reasons which will be discussed shortly, we will adopt this solution for the intermediate region, but we will assume a small value for α. Such a choice of α will make the overall stress field close to Hutchinson's prediction which, as noted earlier appears to agree with other calculations, Hutchinson (1968). In fact, the uniform field in the wedge-like region differs only slightly from $T_{11} = k$, $T_{22} = 2k$ when α is small.

2.3 Matching of stress fields

In order to obtain a complete picture of the crack-line stresses, we have to match the stress fields in the near-tip zone to the ones in the intermediate region. The simplest way of achieving this is to extend the near tip solution (2.7) until the condition $T_{11} = k$, $T_{22} = 2k$ is met. Equation (2.7a) shows that this condition is satisfied at

$$\frac{r}{a} = \kappa = (\sqrt{3}\, e^{\pi/2\sqrt{3}})^{\frac{1}{2}} \cong 2.07 \quad (\omega = \pi/6) \ . \tag{2.9}$$

One would, of course, expect that $\underset{\sim}{T}$ will develop dependence on ϑ in the transition from the essentially axisymmetric field very close to the tip to the non-axisymmetric one away from the tip. It is beyond the scope of the present paper to analyze this transition rigorously, because this would require more information on the near tip deformation than can be obtained by

Figure 6 shows the elastic-plastic boundary in the x_1-a plane. The "a" coordinate of the intersection of this curve and the line defined by (5.4) on which x_o = constant, defines a function of x_o. We shall choose this function for $G^*(x_o)$ in (5.14). Since this construction of G^* yields

$$G^*(x_o) = a \tag{5.18}$$

on the elastic-plastic boundary, we find from (5.9) and (5.14) that

$$F(x_o) = F_2 \ . \tag{5.19}$$

Continuity of $\partial x_2/\partial X_2$ at $x_1 = \kappa a$ gives by the use of (3.30b), (5.11) and (5.14)

$$\eta^{p-1}\kappa\, e^{q\eta}\, \frac{F_1}{F_2} = \left(\frac{\eta a}{G^*(\eta a)}\right)^p e^{q\eta a/G^*(\eta a)} \ . \tag{5.20}$$

It follows from (5.20) that

$$\frac{G^*(\eta a)}{\eta a} = \gamma \ , \tag{5.21}$$

where γ is the root of the equation

$$\eta^{p-1}\kappa\, e^{q\eta}\, \frac{F_1}{F_2} = \gamma^{-p}\, e^{q/\gamma} . \tag{5.22}$$

Hence, we have

$$G^*(x_o) = \gamma\, x_o . \tag{5.23}$$

Equations (5.14), (5.19) and (5.23) then determine $\partial x_2/\partial X_2$ in $\kappa a < x_1 < x_p$ as

$$\frac{\partial x_2}{\partial X_2} = F_2 \left(\frac{a}{\gamma x_o}\right)^p e^{-qx_o\left(\frac{1}{a} - \frac{1}{\gamma x_o}\right)} \ . \tag{5.24}$$

6. Results

On the crack line the near-tip region corresponds to $a \leq x_1 \leq \kappa a$, where κ is given by (2.9): $\kappa = 2.07$. Equation (3.28) relates X_1 to x_1 by

$$X_1 = F(ae^{-g(\rho)}) = \frac{\eta}{F_1} ae^{-g(\rho)} \quad , \tag{6.1}$$

where (5.11) has been used and $g(\rho)$ is defined by (3.26). Here ρ should be interpreted as $\rho = x_1/a$, and η is given by (5.6b). For $x_1 = \kappa a$, (6.1) yields $X_1 = \eta a/F_1$. At $x_1 = a$ we have $\rho = 1$ and (6.1) yields $X_1 = 0$, because $f(1) = 1$, and hence $g(\rho) \sim [f'(1)-1]^{-1} \ell n(\rho-1)$ as $\rho \downarrow 1$, which implies $\exp[-g(\rho)] \sim (\rho-1)^{2/3}$ as $\rho \downarrow 1$, because (3.9) and (3.10) give $f'(1) = -\frac{1}{2}$.

The crack-line stresses in the near-tip zone are given by (3.4c,d) and (2.7b,c). Thus,

$0 \leq X_1 \leq \eta a/F_1$, or $a \leq x_1 \leq \kappa a$:

$$T_{11} = 2k\cos(\omega + \pi/6), \quad T_{22} = 2k\cos(\omega-\pi/6) \quad , \tag{6.2a,b}$$

where $\pi/6 \leq \omega \leq \pi/3$, and according to (2.7a) x_1 and ω are related by

$$\left(\frac{x_1}{a}\right)^2 = \frac{\sqrt{3}}{2\sin\omega} e^{\sqrt{3}(\pi/3-\omega)} \quad . \tag{6.3}$$

The deformation gradients on the crack line follow from (3.29):

$$\frac{\partial x_1}{\partial X_1} = \frac{F_1}{\eta} [\rho-f(\rho)]e^{g(\rho)} \quad , \tag{6.4}$$

$$\frac{\partial x_2}{\partial X_2} = \rho \frac{F_1}{\eta} e^{g(\rho)} \quad . \tag{6.5}$$

At $x_1 = a$, $\partial x_2/\partial X_2$ is singular, but $\partial x_1/\partial X_1$ vanishes.

The intermediate region is defined by $\kappa a \leq x_1 \leq x_p$. The corresponding range of X_1 follows from (5.12) as $\eta a/F_1 \leq X_1 \leq (x_p - \sqrt{3}a/\kappa)/F_1$. The crack-line stresses in the intermediate region are given by (2.10). Thus

$\eta a/F_1 \leq X_1 \leq (x_p - \sqrt{3}/\kappa)/F_1$, or $\kappa a \leq x_1 \leq x_p$:

$$T_{11} = k \ , \quad T_{22} = 2k \ . \tag{6.6a,b}$$

From (5.12) we conclude

$$\frac{\partial x_1}{\partial X_1} = F_1 \ , \tag{6.7}$$

while $\partial x_2/\partial X_2$ is given by (5.24).

The computation of numerical results requires the evaluation of the integral in (3.26), where $f(\rho)$ follows from either (3.13) or (3.15) and (2.7a). The precise evaluation of the integral, which is not difficult numerically, may not be worth the effort considering the approximate nature of the present analysis. Hence, we will simplify the analysis by using the approximate formula (3.15) for f. In addition it is found that the Hermitian interpolation f^* of f

$$f^* = -L(\rho-1)(\rho^2+C_1\rho + C_2) + \rho \ , \tag{6.8}$$

is a sufficiently accurate approximation for f, where

$$C_1 = -\frac{2\{\kappa^3 - 4\kappa^2 - (1-3\sqrt{3})\kappa + \sqrt{3}\}}{\kappa^2 - 5\kappa + 4\sqrt{3}}, \tag{6.9a}$$

$$C_2 = \frac{3\kappa^4 - 7\kappa^3 + 6\sqrt{3}\kappa - 2\sqrt{3}}{\kappa^2 - 5\kappa + 4\sqrt{3}}, \tag{6.9b}$$

$$L = \frac{3}{2(1+C_1+C_2)} . \tag{6.9c}$$

It is noted that this approximation will predict the correct singularity for deformation gradients at the crack tip because of the use of Hermitian interpolation. Indeed, as was seen earlier, the singularity of $\partial \underset{\sim}{x}/\partial \underset{\sim}{X}$ is determined by the derivative of f at $\rho = 1$. Also, it is evident, from (3.8), that the singularity of $\partial \underset{\sim}{x}/\partial \underset{\sim}{X}$ does not depend on δ. This observation serves as another justification for the use of (3.15). With f^* replacing f in (3.26), we obtain

$$\frac{\partial x_1}{\partial X_1} = \frac{F_1 L}{\eta} [(\kappa-1)^2(\rho-1)]^{1/3}(\rho^2+C_1\rho + C_2)\left|\left(\frac{\kappa-\omega_o}{\rho-\omega_o}\right)^{\beta_o}\right|^2, \tag{6.10}$$

$$\frac{\partial x_2}{\partial X_2} = \frac{F_1}{\eta} \rho \left(\frac{\kappa-1}{\rho-1}\right)^{2/3} \left|\left(\frac{\kappa-\omega_o}{\rho-\omega_o}\right)^{\beta_o}\right|^2, \tag{6.11}$$

where

$$\omega_o = \frac{-C_1+i\ (4C_2-C_1^2)^{\frac{1}{2}}}{2}, \quad \beta_o = -\frac{1}{3} + i\ \frac{C_1+2}{3\ (4C_2-C_1^2)^{\frac{1}{2}}} . \tag{6.12a,b}$$

We also have

$$X_1 = \frac{a}{F_1}\left(\frac{\rho-1}{\kappa-1}\right)^{2/3} \left|\left(\frac{\rho-\omega_o}{\kappa-\omega_o}\right)^{\beta_o}\right|^2 . \tag{6.13}$$

Hence we have

$$\frac{\partial x_2}{\partial X_2} = \frac{\rho a}{X_1} \quad . \tag{6.14}$$

Further simplifications may be introduced when $\delta = k/2\mu << 1$. Then

$$F_{1,2} \cong 1 + O(\delta) \cong 1 \ , \quad p \cong 3/\kappa^4 \cong 0.16, \quad q = \sqrt{3}/\kappa^3 \cong 0.19. \tag{6.15a,b,c}$$

With these constants, (5.22) gives

$$\gamma = 0.321. \tag{6.16}$$

This result, (5.4), (5.23) and (5.18) yield $x_p = 3.95a$ and from (5.12), we see that the material in the range $0 < X_1 < 3.12a$ will be in plastic zone. Plots of the deformation gradients on the crack line for $\delta = 0$ are given in Fig. 7.

Finally, we can make an estimate of a in terms of the stress intensity factor K_I of linear elastic fracture mechanics by equating the plastic zone sizes predicted by the present theory and existing small strain theories. Small strain theories predict that the length of the plastic zone x_p is given by

$$x_p = c\, K_I^2/k^2 \ , \tag{6.17}$$

where $c = \pi/24 \cong 0.13$ according to the Dugdale model, and $c = 2\sqrt{2}/9\pi \cong 0.10$, according to the analysis Achenbach and Dunayevsky (1984). By equating (6.17) to $x_p - a = 2.95a$ and $X_p = 3.12a$ respectively, we obtain

$$a \cong \frac{c}{2.95}\frac{k_I^2}{k^2} \text{ and } a \cong \frac{c}{3.12}\frac{k_I^2}{k^2} \quad . \tag{6.18a,b}$$

Acknowledgment

This work was carried out in the course of research sponsored by the U.S. Office of Naval Research (Contract No. N00014-76-C-0063).

References

Achenbach, J.D. and Dunayevsky,V.	1984	J. Mech. Phys. Solids 32, 89.
Achenbach, J.D. and Li, Z.	1984	Eng. Fracture Mech. 20, 535.
Dienes, J.K.	1979	Acta Mech. 32, 217.
Hutchinson, J.W.	1968	J. Mech. Phys. Solids 16, 337.
Kachanov, L.M.	1971	Foundations of the Theory of Plasticity, North Holland, Amsterdam.
Knowles, J.K.	1977	Int. J. Fracture 13, 611.
Knowles, J.K. and Sternberg, Eli	1980	J. Elasticity 10, 81.
Knowles, J.K. and Sternberg, Eli	1981	J. Elasticity 11, 129.
Knowles, J.K. and Sternberg, Eli	1983	J. Elasticity 13, 257.
Lee, E.H., Mallett, R.L. and Wertheimer, T.B.	1983	J. Appl. Mech. 50, 554.
Lo, K.K.	1977	Int. J. Solids Structures 13, 1219.
McMeeking, R.M.	1977	J. Mech. Phys. Solids 25, 357.
Rice, J.R. and Johnson, M.A.	1970	Inelastic Behavior of Solids, (edited by Kanninen, M.F., Adler, W.F., Rosenfield, A.R. and Jaffee, R.I.), p. 641. McGraw-Hill, New York.
Rice, J.R., McMeeking, R.M., Parks, D.M. and Sorensen, E.P.	1979	Comp. Meth. Appl. Mech. Eng. 17/18, 411.
Thomason, P.F.	1979	Fracture Mechanics in Engineering Application (edited by Sih, G.C. and Valluri, S.R., p. 43. Sijthoff & Noordhoff, The Netherlands.

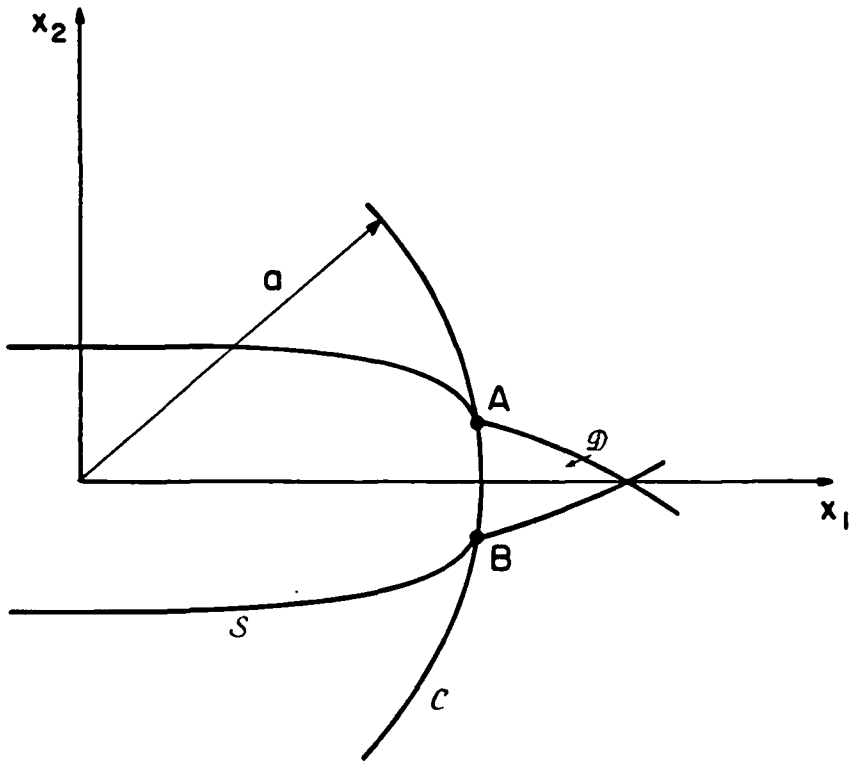

Fig. 1 Crack-tip geometry

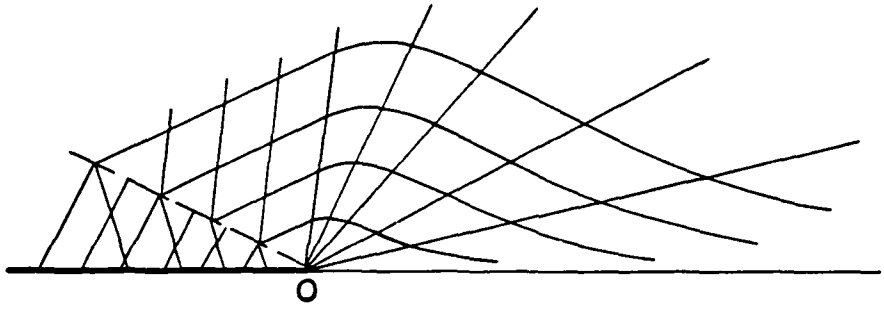

Fig. 2 Characteristic curves for Hutchinson's field. Point 0 corresponds to the crack tip.

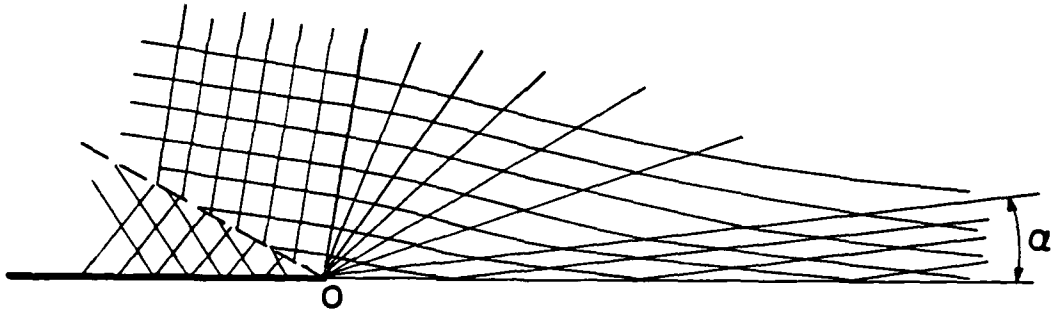

Fig. 3 Characteristic curves for Thomason's field. Point 0 corresponds to the crack tip.

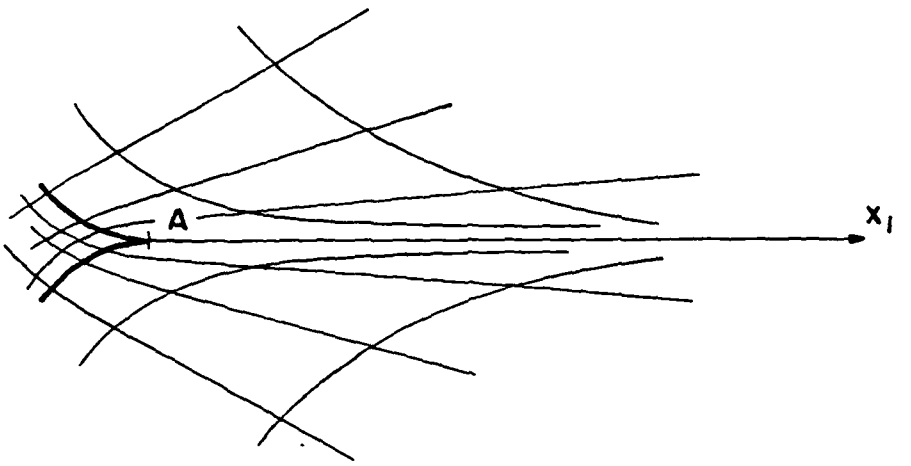

Fig. 4 Characteristic curves for crack-tip zone and intermediate region, with Hutchinson's field in intermediate region.

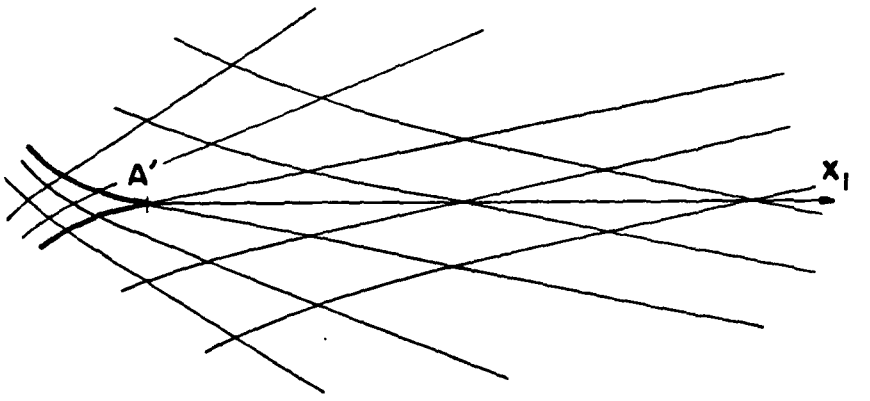

Fig. 5 Characteristic curves for crack-tip zone and intermediate region, with Thomason's field in intermediate region

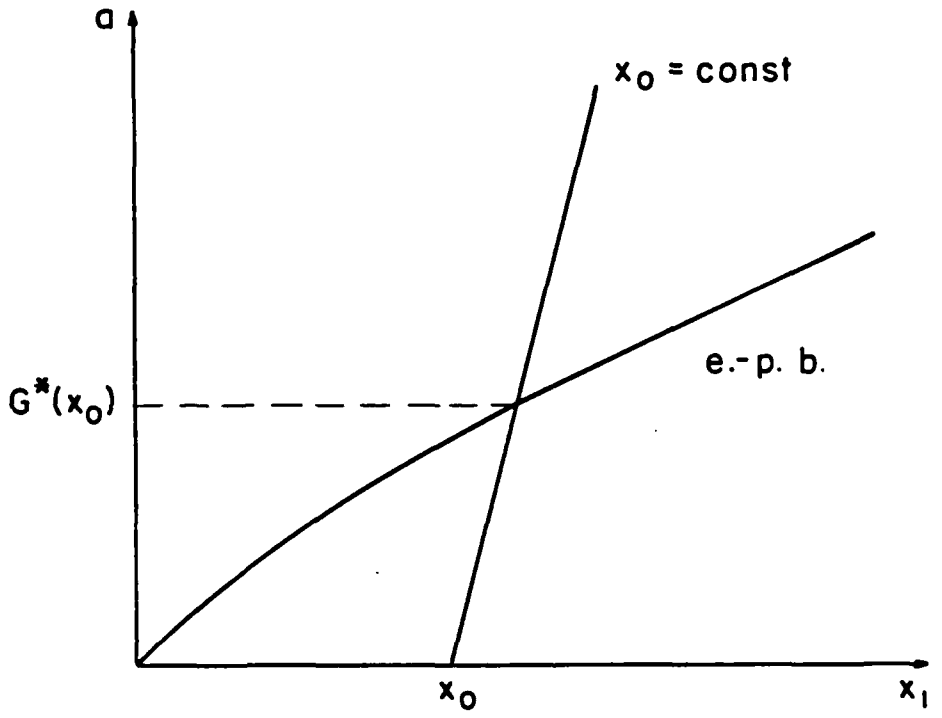

Fig. 6 Elastic-plastic boundary in x_1-a plane.

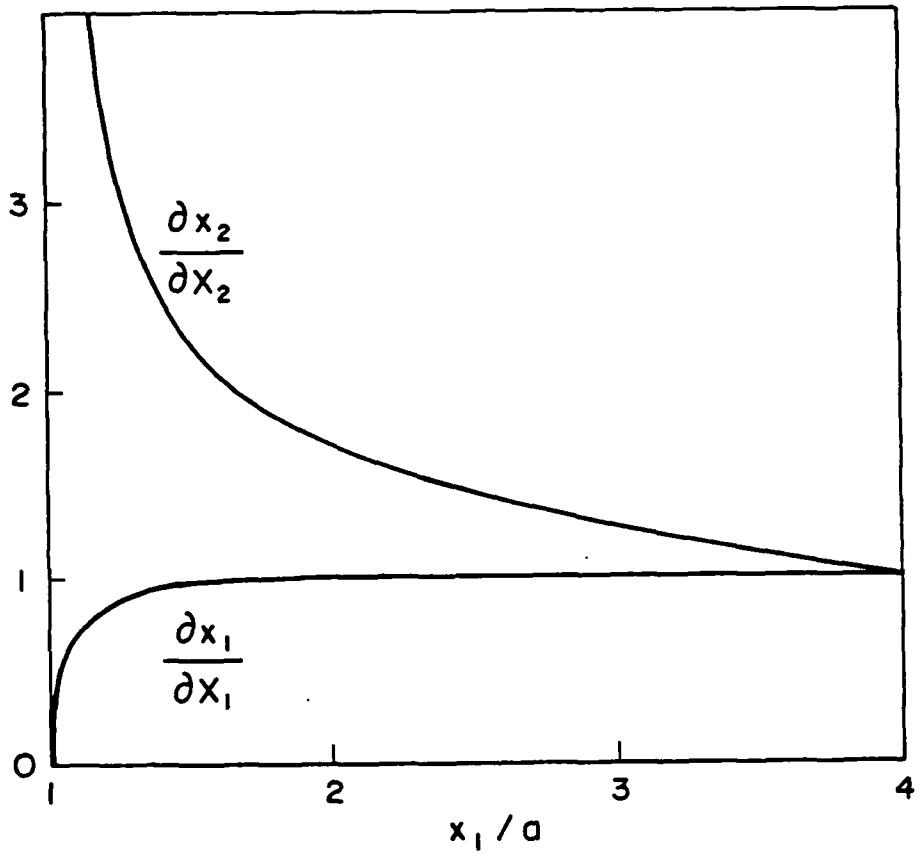

Fig. 7 Deformation gradients versus x_1/a

REPORT DOCUMENTATION PAGE

READ INSTRUCTIONS BEFORE COMPLETING FORM

UMBER: -TR-85-2	2. GOVT ACCESSION NO.
3. RECIPIENT'S CATALOG NUMBER	
Subtitle): Deformation Crack-Line Fields in a Elasto-Plastic Sheet	5. TYPE OF REPORT & PERIOD COVERED: Interim
	6. PERFORMING ORG. REPORT NUMBER
shimura and J. D. Achenbach	8. CONTRACT OR GRANT NUMBER(s): N00014-76-C-0063
NG ORGANIZATION NAME AND ADDRESS: Western University, Evanston, IL 60201	10. PROGRAM ELEMENT, PROJECT, TASK AREA & WORK UNIT NUMBERS
LING OFFICE NAME AND ADDRESS: e of Naval Research; ural Mechanics Department; ment of the Navy, Arlington, VA 22217	12. REPORT DATE: February 1985
	13. NUMBER OF PAGES: 37
ING AGENCY NAME & ADDRESS(if different from Controlling Office)	15. SECURITY CLASS. (of this report): Unclassified
	15a. DECLASSIFICATION/ DOWNGRADING SCHEDULE

TION STATEMENT (of this Report)

oved for public release; distribution unlimited.

TION STATEMENT (of the abstract entered in Block 20, if different from Report)

IENTARY NOTES

DS (Continue on reverse side if necessary and identify by block number)

te deformation
I
e stress
ect plasticity
in field

T (Continue on reverse side if necessary and identify by block number)

inite deformation in the crack-tip zone of plastic deformation is igated for Mode-I opening of a crack in a thin sheet of elasto-plastic al. The material obeys the von Mises yield criterion in the true es, and the stretching tensor satisfies a flow law of the Prandtl- type. Incompressibility and a state of generalized plane stress are d. It is assumed that linearized elasticity applies outside the zone stic deformation. On the crack line between the crack tip and the

elastic-plastic boundary, two distinct regions have been recognized: the near tip zone and the intermediate region. In the near tip zone the fields are controlled by the radius of curvature of the blunted crack tip. Here the stress field has been approximated by classical plane stress results. It has been assumed that the crack-line stresses may be taken as uniform in the intermediate region. In each region, deformation variables have been determined by the use of the constitutive relations, and the results have been matched to the corresponding quantities in the neighboring region(s). In this manner expressions have been constructed for the deformation gradients on the crack line, in terms of the distance to the crack tip in the deformed configuration, the yield stress in shear and the stress-intensity factor of linear elastic fracture mechanics.

END

FILMED

8-85

DTIC

END

FILMED

8-85

DTIC